


Article

# 3D-Printed Solid Dispersion Drug Products

Suet Li Chew<sup>1</sup>, Laura Modica de Mohac<sup>1,2</sup> and Bahijja Tolulope Raimi-Abraham<sup>1,\*</sup> 

<sup>1</sup> Drug Delivery Group, Institute of Pharmaceutical Science, Faculty of Life Sciences and Medicine, King's College London, Franklin-Wilkins Building, 150 Stamford Street, London SE1 9NH, UK; suet.chew@kcl.ac.uk (S.L.C.); laura.1.modica\_de\_mohac@kcl.ac.uk (L.M.d.M.)

<sup>2</sup> Department of Sciences for Health Promotion and Mother-Child Care "G. D'Alessandro", University of Palermo, 90100 Palermo, Italy

\* Correspondence: Bahijja.Raimi-Abraham@kcl.ac.uk; Tel.: +020-7836-5454

Received: 14 October 2019; Accepted: 5 December 2019; Published: 11 December 2019



**Abstract:** With the well-known advantages of additive manufacturing methods such as three-dimensional (3D) printing in drug delivery, it is disappointing that only one product has been successful in achieving regulatory approval in the past few years. Further research and development is required in this area to introduce more 3D printed products into the market. Our study investigates the potential of fixed dose combination solid dispersion drug products generated via 3D printing. Two model drugs—fluorescein sodium (FS) and 5-aminosalicylic acid (5-ASA)—were impregnated onto a polyvinyl alcohol (PVA) filament, and the influence of solvent choice in optimal drug loading as well as other influences such as the physicochemical and mechanical properties of the resultant filaments were investigated prior to development of the resultant drug products. Key outcomes of this work included the improvement of filament drug loading by one- to threefold due to solvent choice on the basis of its polarity and the generation of a 3D-printed product confirmed to be a solid dispersion fixed dose combination with the two model drugs exhibiting favourable in vitro dissolution characteristics.

**Keywords:** 3D printing; amorphous solid dispersion; additive manufacturing; poor solubility; fixed dose combination

## 1. Introduction

A fixed-dose combination (FDC) product is a single dosage form that incorporates two or more active pharmaceutical ingredients (APIs) [1,2]. Between 2013 and 2018, the European Medicines Agency (EMA) approved 66 FDCs, most of which were antiretrovirals for human immunodeficiency virus (HIV) infections [3]. FDC products have several advantages over conventional medicinal products, namely, greater efficacy (43%,  $n = 33$ ) and compliance (18%,  $n = 14$ ) [4–7]. However, disadvantages have been highlighted, such as a reduction in medication adherence (24%–26%) in some cases [8,9].

The use of three-dimensional (3D) printing in drug delivery is still in its infancy compared to traditional technologies; however, research and development is rapidly expanding in this area due to the benefits of 3D printing to develop personalized patient-specific dosage forms with tailored release profiles [10–13]. Traditional powder direct compression techniques to generate FDC medicinal products is not suitable [14–19]. Currently, the only regulatory approved (by the Food and Drug Administration (FDA)) 3D printed medicinal product is the oro-dispersible levetiracetam tablet, Spritam developed by Aprelia Pharmaceuticals in 2015 [20]. The number of regulatory approved 3D printed drug products remains limited due to the number of printers available to comply with good manufacture practice (GMP), high variability of 3D printers, and end product quality [21–24]. Fused deposition modelling (FDM) uses heat to melt thermoplastic polymers into the molten state and the object to be printed is designed by computer-aided drafting, which enables it to be printed layer-by-layer as the printer nozzle

deposits the extrudate [15,25]. FDM 3D printing has been explored extensively in the development of medicinal products and, more specifically, FDC products. FDM 3D printing is capable of producing drug products with multiple active pharmaceutical ingredients in various compartments, which is advantageous in developing patient-centric formulations to reduce multiple daily dosing, therefore improving patient compliance and therapeutic efficiency [26–28].

The use of solid dispersion technology has been explored in FDM 3D printing [26]. In the study described here, we firstly explored the influence of solvent type on filament (polyvinyl alcohol (PVA)) drug loading using the drug impregnation method. We then manufactured solid dispersion FDC 3D printed dosage forms using the drug-solvent-filament combination, which gave the highest drug loading. Physicochemical characterization of the filaments was conducted and an evaluation of filament and FDC mechanical properties by way of hardness and tensile strength were also evaluated. In vitro drug dissolution studies on the FDC 3D printed dosage forms were also conducted [29,30].

Several studies have used the drug impregnation method to load drugs onto polymer filaments for 3D printing. In the case of PVA filaments, this is commonly done by soaking the filament in a highly saturated drug solution. However, this method can result in low drug-loading (<2% *w/w*) due to slow drug diffusion into polymer [17,24,29–31]. The general drug-loading differences using different solvents such as ethanol (EtOH) and methanol (MeOH) for this filament drug loading method still remains relatively unknown. Studies conducted on 3D-printed FDC often separate APIs into different compartments such as the DuoCaplet design by Goyanes et al. [23]. The potential of FDM-printed monolithic FDC design, by incorporating two APIs into the same polymer filament, is yet to be investigated in terms of ability to independently tailor the different APIs release. This study aimed to explore the potential of increasing drug-loading efficiency by altering solvent choice, and to study the in vitro dissolution profiles of the FDM-printed monolithic FDC tablet developed. Fluorescein sodium (FS) and 5-aminosalicylic acid (5-ASA) were chosen as model drugs due to their proven FDM-printability [29,30]. PVA was selected as main polymer as it is the only commercially extruded polymer filament that would dissolve in vivo [29].

## 2. Materials and Methods

### 2.1. Materials

Fluorescein sodium salt (FS, 376.27 g/mol, decomposition temperature = 315–395 °C), absolute ethanol, and methanol ≥99.8% were manufactured by Sigma-Aldrich, United Kingdom. Dimethyl sulfoxide (DMSO) was purchased from Honeywell. 5-Aminosalicylic acid (5-ASA, 153.14 g/mol, decomposition temperature = 280 °C) purchased from FLUKA was donated by University College London School of Pharmacy. Polyvinyl alcohol (PVA) filament, 1.75 mm diameter, was purchased from RS-Pro. Phosphate buffer (pH 6.8) tablets were purchased from Millipore Corporation.

### 2.2. Methods

#### 2.2.1. Filament Preparation

Drug-containing filaments were prepared using the method described by Goyanes et al. [29,30]. In brief, 5 m of PVA filament was soaked in the drug-solvent mixture (100 mL) and stirred magnetically at 470 rpm for 24 h. The drug-loaded filaments were then heated (60 °C) in an oven (Pickstone Ovens, Island Scientific, Isle of Wight, UK) to facilitate rapid solvent evaporation (≈2 h). Resultant filaments were protected from light and moisture with aluminum foil and desiccants, respectively. Tagami et al. [31] suggested that this method of drug load requires the use of a saturated drug solution. Therefore, the drug concentrations chosen were based on drug concentrations (of FS and 5-ASA) used in previous studies [29,30]. Table 1 outlines the solvents, drug choices, and concentrations for the preparation of drug-loaded and solvent-soaked filaments. The names of the filament samples are included in brackets.

**Table 1.** Solvent, drug, and drug concentrations used.

Active Pharmaceutical Ingredient (API)	Ethanol (EtOH)	Methanol (MeOH)	Dimethyl Sulfoxide (DMSO)
	PVA		
Fluorescein sodium (FS)	2.0% <i>w/v</i> (FS-EtOH)	2.5% <i>w/v</i> (2.5%FS-MeOH)	2.5% <i>w/v</i> (FS-DMSO)
5-aminosalicylic acid (5-ASA)	1.0% <i>w/v</i> (5-ASA-EtOH)	1.25% <i>w/v</i> (5-ASA-MeOH)	1.25% <i>w/v</i> (5-ASA-DMSO)
FS and 5-ASA		2.5% <i>w/v</i> FS and 1.25% <i>w/v</i> 5-ASA (FDC-MeOH)	

## 2.2.2. Solid State Characterization of Filaments

### X-Ray Powder Diffraction

Structural characterization of filaments produced was conducted using a D/Max-BR diffractometer (RigaKu, Tokyo, Japan) with Cu K $\alpha$  radiation operating at 40 kV and 15 mA (Cu K $\alpha$  radiation) over the 2 $\theta$  range 10–50° with a step size of 0.02° at 2°/min.

### 2.2.3. 3D-Printed Drug Product Design and Optimization

Tablets were designed using TinkerCAD and were then imported as stl. format into MakerBot Desktop Beta (V3.10.1.1389) (MakerBot Industries, Brooklyn, NY, USA). Tablets were printed with PVA filament and drug loaded filaments using a MakerBot Replicator 2X (MakerBot Inc., Brooklyn, NY USA) with the following dimensions 10.45 × 10.54 × 1.2 mm [30]. Printer settings were standard resolution, 230 °C extrusion and 20 °C platform temperature, 100% hexagonal infill with raft option deactivated when printing drug-loaded tablets but activated for blank PVA tablets [24]. Printed tablets were assessed for weight uniformity.

### 2.2.4. Morphology Studies

#### Scanning Electron Microscopy

Hitachi S5000 Emission Gun (FEG) (Hitachi, Maidenhead, UK) with Tungsten Tip (25 kV) was used to examine gold-coated (10 nm thickness) PVA tablet. Images were captured using secondary electron detector from ×70 to ×10.9 K magnification.

### 2.2.5. Crushing Strength

The crushing strength tests were conducted using a C50 Tablet Hardness and Compression tester (Engineering System, Nottingham, United Kingdom) on PVA and drug-loaded filaments. Figure 1 shows the sample orientation in the tester. Filament hardness was recorded as mean crushing strength (kg).

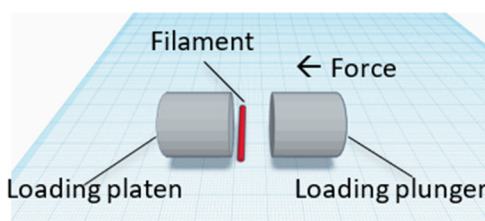


**Figure 1.** Orientation of filaments between loading plunger and platen. Increasing force was applied by loading plunger towards the platen. Direction of force is indicated by the arrow (←).

## 2.2.6. Solubility, Drug Content, and In Vitro Drug Dissolution Studies

### Solubility Studies

Solubility studies were conducted on FS and 5-ASA dissolved in the in vitro dissolution media, pH 6.8 phosphate buffer, and PVA solutions. Different amounts of PVA filament were dissolved in pH 6.8 phosphate buffers to prepare PVA-pH 6.8 solutions. Excess API (either FS or 5-ASA) was added to PVA solutions and vigorously stirred for 72 h at  $37 \pm 0.5$  °C at 150 rpm. The saturated solutions were then filtered using a 0.45 µm membrane, and the API concentration in the filtrate was determined spectrophotometrically at 330 nm for 5-ASA and 490 nm for FS.

### Calculation of Drug Content in PVA Filaments

Drug-loaded filaments were dissolved in pH 6.8 phosphate buffer and assayed spectrophotometrically (Perkin Elmer Lambda 35 Spectrophotometer) (PerkinElmer, Inc. Waltham, MA, USA) at 330 nm for 5-ASA and 490 nm for FS. PVA did not interfere with the UV analysis. Drug content was calculated using Equation (1) below.

$$\text{Drug - content (\% w/w)} = \left( \frac{\text{Weight of drug (g)}}{\text{Weight of filament (g)}} \right) \times 100 \quad (1)$$

### In Vitro Drug Dissolution Studies

In vitro dissolution studies were conducted in pH 6.8 phosphate buffer (small intestine) at  $37 \pm 0.5$  °C and a rotational speed of 100 rpm under non-sink conditions to observe any supersaturation effect from the solid dispersion products generated. At predetermined intervals, samples were withdrawn and filtered through a 0.45 µm filter and the filtrate was analysed spectrophotometrically at 330 nm for 5-ASA and 490 nm for FS.

## 2.2.7. Statistical Analysis

Unpaired two-tailed *t*-test was performed using SigmaPlot V14.0 (Systat Software Inc. Berkshire, UK) with 95% significance level.  $p < 0.05$  was regarded as significant.

## 3. Results

### 3.1. Solvent Choice Optimization

Solvents of increasing polarity: DMSO < EtOH < MeOH were investigated for their drug-loading efficiency into PVA filaments. Model drugs FS and 5-ASA are both polar; dissolving in solvents of higher polarity allows for generation of a larger concentration gradient for drug diffusion into the polymer (PVA) filament, therefore giving higher drug-loading in the presence of solvents of a higher polarity [32,33].

Table 2 shows mean drug content of the drug-impregnated filaments. DMSO completely solubilized PVA; therefore, the results below are based only on EtOH and MeOH. Coefficient of variation (%CV) ranged from 0.2% to 13.5%, highlighting the issue of non-uniform drug loading with soaking method, requiring further soaking apparatus choice selection.

**Table 2.** Mean drug-content (% w/w) of drug-loaded filaments prepared via drug impregnation method.

Solvents	Drug-Loaded Filaments	Drug Loading (% w/w)
Ethanol	FS-EtOH	1.19 ± 0.161
	5-ASA-EtOH	0.10 ± 0.001
Methanol	FS-MeOH	4.89 ± 0.449
	5-ASA-MeOH	0.17 ± 0.007
	FDC-MeOH	FS: 6.16 ± 0.197
		5-ASA: 2.97 ± 0.362

Comparing single-drug-loaded filaments, MeOH was found to significantly increase drug loading compared to EtOH, irrespective of drugs ( $p < 0.05$ ), fitting the hypothesis. The ratio of FS drug loading between MeOH and EtOH was approximately 4:1, whereas the ratio was smaller but statistically significant for 5-ASA (approximately 1.5:1 between MeOH and EtOH). Despite using the same drug concentration, 5-ASA content in FDC-MeOH filament was significantly higher ( $\approx 17$  fold) than 5-ASA content in 5-ASA-MeOH filament ( $p < 0.01$ ). MeOH was chosen to prepare FDC filament for the rest of the study due to its improved drug loading.

### 3.2. Filament Characterization

#### 3.2.1. Filament Hardness

It is expected that filament mechanical properties, hardness in particular, will change after drug impregnation, especially as most of the solvents used have the potential to degrade PVA [23]. Changes to filament properties can influence printability [34]. The crushing strength is frequently used in the pharmaceutical industry to describe the resistance of tablets to the application of a compression load [35]. In this study, we used the crushing strength to provide an indication of the changes in filament strength after soaking in EtOH and MeOH. Interestingly, the PVA filament crushing strength (kg) of  $46.13 \pm 0.89$  kg decreased when the PVA filament was soaked (without the presence of the APIs) in EtOH and MeOH to  $10.25 \pm 1.04$  kg and  $10.78 \pm 0.48$  kg, respectively. For single-drug-loaded filament, both FS-EtOH and 5-ASA-EtOH filaments had crushing strengths of  $14.93 \pm 1.74$  kg and  $14.65 \pm 0.81$  kg, respectively, however, these values significantly increased ( $p < 0.01$ ) for MeOH-loaded drug filaments, FS-MeOH ( $25.34 \pm 1.52$  kg), and 5-ASA-MeOH ( $22.78 \pm 1.21$  kg). The crushing strength of FDC-MeOH filament was  $16.77 \pm 1.12$  kg, similar to API-EtOH filaments ( $p > 0.05$ ).

#### 3.2.2. Solid State Characterization of Filaments

X-Ray Powder Diffraction (XRPD) studies were conducted to determine any potential physico-chemical changes to the API such as crystalline-amorphous transformation. XRPD diffractograms of raw materials of 5-ASA (Figure 2A) and FS (Figure 2B) both showed characteristic Bragg's peaks, as confirmed by Groom et al. and Banic-Tomasic et al. [36,37]. XRPD studies on PVA filament, (Figure 2C) PVA-MeOH (Figure 2D), and FDC-MeOH filament (Figure 2E) showed characteristic amorphous halo with no evidence of crystalline API peaks.

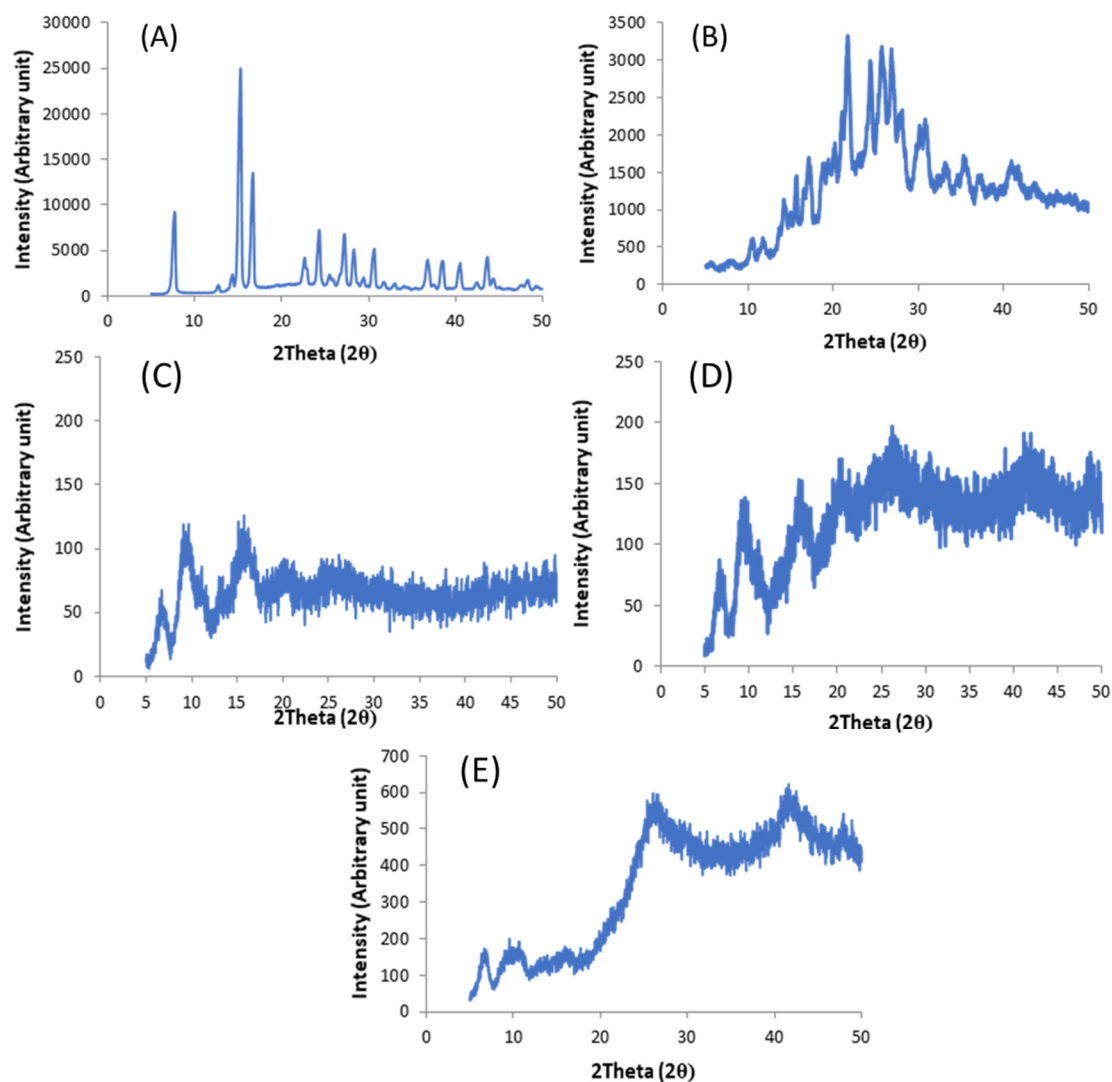


**Figure 2.** X-ray powder diffractograms of (A) 5-ASA, (B) FS, (C) blank polyvinyl alcohol (PVA) filament, (D) PVA-MeOH filament, and (E) FDC-MeOH filament data. Samples were scanned from 10–50° 2 $\theta$  (stepwise: 0.02°, at 2°/min). Please note that different  $y$ -axis scales were used.

### 3.3. Characterization of 3D-Printed Dosage Forms

#### Morphology Studies

Layer-by-layer building of object via molten polymer fusion onto previously solidified extrudate layer during printing was expected to give extrudate-stacking appearance [38]. SEM images of a representative 3D printed dosage form is shown in Figure 3. Figure 3 clearly shows multiple voids on the dosage form surface, moreover, the dosage form obtained shows extrudate-stacking as expected and previously identified with FDM-printed dosage forms [25]. Representative images of printed products are provided in Figure 4.



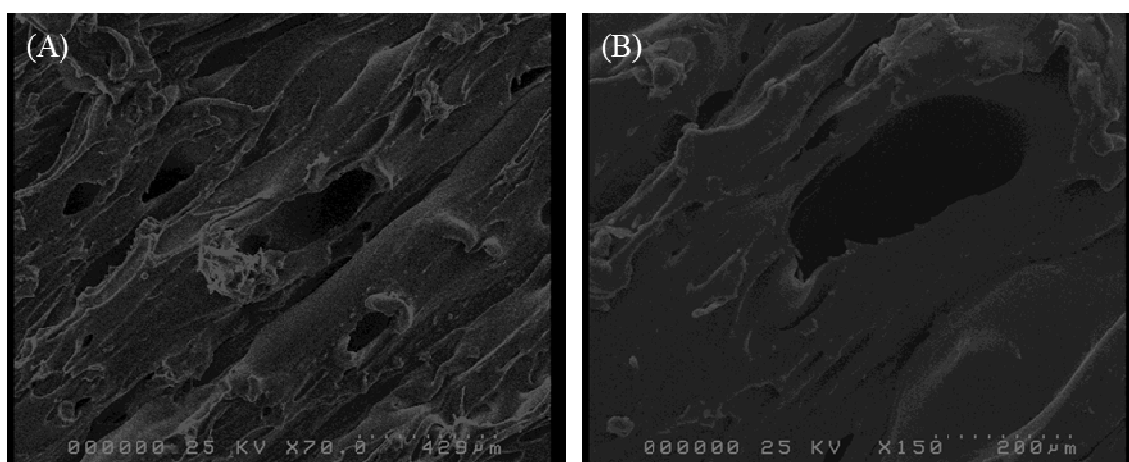


**Figure 3.** Surface morphology of PVA tablet (top view) at (A)  $\times 70$  and (B)  $\times 150$  magnification.

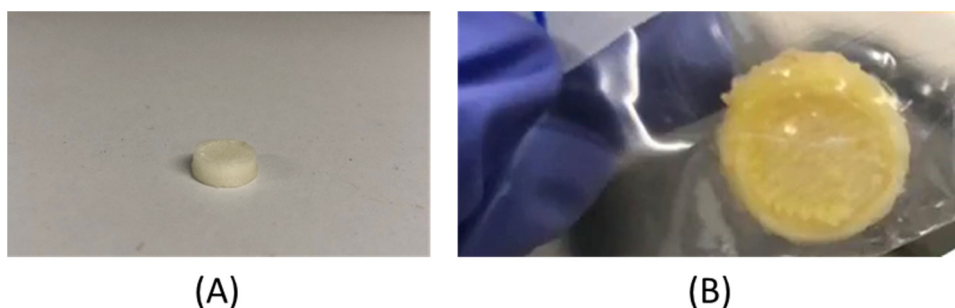


**Figure 4.** Representative image (A) printed PVA product and (B) three-dimensional (3D)-printed fixed-dose combination (FDC) drug product with dimensions  $10.45 \times 10.54 \times 3.79$  mm.

#### 3.4. In Vitro Dissolution

Saturated solubility of FS and 5-ASA was determined in in vitro dissolution medium at increasing PVA concentration. FS and 5-ASA saturated solubility in pH 6.8 phosphate buffer was 385.82 and 2.98 mg/mL, respectively. In the presence of increased PVA concentration (0.6% *w/v* and 0.4% *w/v*), FS and 5-ASA saturated solubility was 465.75 and 1.60 mg/mL, respectively.

FS and 5-ASA raw materials achieved complete dissolution within 5 min (data not shown); therefore, Figure 5 shows dissolution profiles of the 3D-printed FDC-MeOH product. Amorphous solid dispersion (ASD) formulations are known to experience rapid dissolution before recrystallizing at a rate corresponding to PVA concentration, acting as a crystallization inhibitor [39–41]. The 3D-printed FDC-MeOH product dissolution showed characteristic ASD spring-and-parachute dissolution profile of both FS and 5-ASA. Peak concentration was achieved at  $t = 30$  min for 5-ASA ( $8.36 \pm 0.06$   $\mu\text{g/mL}$ ), corresponding to a dissolution rate of 16.71  $\mu\text{g/mL/h}$  and  $t = 45$  min for FS ( $19.24 \pm 0.24$   $\mu\text{g/mL}$ ).

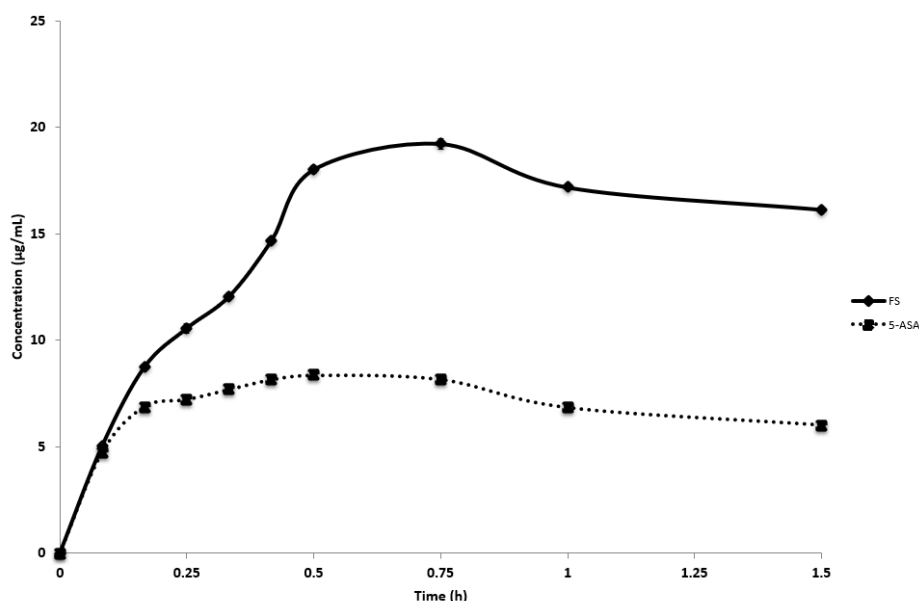


**Figure 5.** In vitro dissolution profile of 3D-printed FDC-MeOH dosage form in phosphate buffer pH 6.8. Error bars representing standard deviations.

#### 4. Discussion

The main aim of this study was to investigate the effect of different solvent in loading drugs on printable PVA filament. The impregnation method used has already been used in studies by Goyanes et al. where drug contents for 5-ASA- and FS-loaded PVA filaments were  $0.063 \pm 0.001\%$  *w/w* and  $0.29 \pm 0.01\%$  *w/w*, respectively [29,30]. In our study, we were able to achieve approximately three-fold and one-fold higher FS and 5-ASA drug-loading, respectively, compared to the studies of Goyanes et al. In particular, it was noted that MeOH-loaded drug filaments had significant improvement in drug-loading of polar FS and 5-ASA compared to EtOH, highlighting the importance of matching solvent drug polarity when using the drug impregnation method. Apart from solvent polarity, drug dielectric constant, solubility, as well as temperature and hygroscopicity can affect drug loading [42]. The presence of FS may have altered MeOH dielectric constant, facilitating H<sup>+</sup> ion dissociation from 5-ASA, and increasing 5-ASA solubility in MeOH; this proposed synergistic effect requires further investigation [43–46].

Our findings on changes in filament hardness before and after drug impregnation showed that drug and solvent molecules can interpose between polymer chains, weakening polymer–polymer interaction and increasing chains movements, resulting in reducing PVA filament hardness by more than 50% after drug-loading and solvent-soaking [47–49]. Because plasticizing effect has previously been found to increase with plasticizer concentration, FDC-MeOH filament, having significantly higher drug loading compared to single-drug filaments, resulted in lower hardness compared to other MeOH-loaded filaments.

The drug dissolution profile of the FDM-printed monolithic FDC tablet (FS and 5-ASA) was evaluated. The advantage of this drug product as a solid dispersion is based on the water-soluble matrix that provides activation energy to drive crystallization [28,50–53]. As drug release from PVA is also regulated by polymer dissolution, all printed tablets in the current study also exhibited spring-and-parachute profile with crystallization inhibited depending on PVA concentration.

The reason for rapid supersaturation resulting in higher maximum concentration could be that the system had insufficient time to induce crystallization when transformation from stable to metastable supersaturation state was quick [54,55]. In the current study, 5-ASA released from the the 3D-printed drug product had initial rapid de-supersaturation; however, the rate declined alongside with the



reduction of 5-ASA in the system. This could be because polymer has a greater precipitation inhibitory effect at lower supersaturation [56–58].

## 5. Conclusions

The use of FDM 3DP technology in the pharmaceutical industry is hindered by several formulation challenges, which the current study aimed to address. This study investigated the solvent influence on optimal drug filament impregnation with an identification that MeOH possessed superior properties compared to EtOH for FS and 5-ASA. Using this method and solvent choice, reasonable drug loading of both FS and 5-ASA onto a single PVA filament was achieved. A 3D-printed solid dispersion FDC drug product was successfully designed and characterized with favourable release profiles and behaviours. Further studies using clinically relevant drugs would be advantageous for the advancement of the work in this area.

**Author Contributions:** Conceptualization, L.M.d.M. and B.T.R.-A.; Methodology, S.L.C., L.M.d.M. and B.T.R.-A.; Software, S.L.C., L.M.d.M. and B.T.R.-A.; Validation, B.T.R.-A.; Formal analysis, S.L.C.; Investigation, S.L.C.; Resources, B.T.R.-A.; Data curation, S.L.C.; Writing—original draft preparation, S.L.C.; Writing—review and editing, L.M.d.M. and B.T.R.-A.; Supervision, L.M.d.M. and B.T.R.-A.; Project administration, L.M.d.M. and B.T.R.-A.

**Funding:** This research received no external funding.

**Acknowledgments:** The authors would like to thank Alvaro Goyanes and Simon Gaisford of University College London (UCL), School of Pharmacy, for providing raw material 5-aminosalicylic acid, and Gareth Williams (UCL, School of Pharmacy) for X-ray powder diffraction results.

**Conflicts of Interest:** The authors declare no conflict of interest.

## References

1. Desai, D.; Wang, J.; Wen, H.; Li, X. Timmins P. Formulation design, challenges, and development considerations for fixed dose combination (FDC) of oral solid dosage forms. *Pharm. Dev. Technol.* **2013**, *18*, 1265–1276. [CrossRef] [PubMed]
2. EMA/CHMP/158268/2017, (CHMP) C for HMP. *Guideline on Clinical Development of Fixed Combination Medicinal Products*. 2017. Available online: [https://www.ema.europa.eu/en/documents/scientific-guideline/guideline-clinical-development-fixed-combination-medicinal-products-revision-2\\_en.pdf](https://www.ema.europa.eu/en/documents/scientific-guideline/guideline-clinical-development-fixed-combination-medicinal-products-revision-2_en.pdf) (accessed on 2 October 2018).
3. Kavanagh, O.N.; Albadarin, A.B.; Croker, D.M.; Healy, A.M.; Walker, G.M. Maximising success in multidrug formulation development: A review. *J. Control. Release* **2018**, *283*, 1–19. [CrossRef] [PubMed]
4. Sawicki-Wrzask, D.; Thomsen, M.; Bjerrum, O.J. An Analysis of the Fixed-Dose Combinations Authorized by the European Union, 2009–2014. *Ther. Innov. Regul. Sci.* **2015**, *49*, 553–559. [CrossRef] [PubMed]
5. Bangalore, S.; Kamalakkannan, G.; Parkar, S.; Messerli, F.H. Fixed-Dose Combinations Improve Medication Compliance: A Meta-Analysis. *Am. J. Med.* **2007**, *120*, 713–719. [CrossRef] [PubMed]
6. FDA. *Fixed Dose Combinations, Co-Packaged Drug Products, and Single-Entity Versions of Previously Approved Antiretrovirals for the Treatment of HIV*; Center for Drug Evaluation and Research (CDER): Rockville, MD, USA, 2006.
7. TheKing’sFund. *Polypharmacy and Medicines Optimisation: Making it Safe and Sound*. Published 2013. Available online: <https://www.kingsfund.org.uk/publications/polypharmacy-and-medicines-optimisation> (accessed on 6 December 2018).
8. Rea, F.; Corrao, G.; Merlino, L.; Mancina, G. Early cardiovascular protection by initial two-drug fixed-dose combination treatment vs. monotherapy in hypertension. *Eur. Heart J.* **2018**, *39*, 3654–3661. [CrossRef] [PubMed]
9. Pourkavoos, N. Unique Risks, Benefits, and Challenges of Developing Drug-Drug Combination Products in a Pharmaceutical Industrial Setting. *Comb. Prod. Ther.* **2012**, *2*, 2. [CrossRef]
10. Jamróz, W.; Szafraniec, J.; Kurek, M.; Jachowicz, R. 3D Printing in Pharmaceutical and Medical Applications—Recent Achievements and Challenges. *Pharm. Res.* **2018**, *35*, 176. [CrossRef]

11. Richey, R.H.; Hughes, C.; Craig, J.V.; Shah, U.U.; Ford, J.L.; Barker, C.E.; Peak, M.; Nunn, A.J.; Turner, M.A. A systematic review of the use of dosage form manipulation to obtain required doses to inform use of manipulation in paediatric practice. *Int. J. Pharm.* **2017**, *518*, 155–166. [[CrossRef](#)]
12. Shastry, B.S. Pharmacogenetics and the concept of individualized medicine. *Pharmacogenom. J.* **2006**, *6*, 16–21. [[CrossRef](#)]
13. Acosta-Vélez, G.F. 3D Pharming: Direct Printing of Personalized Pharmaceutical Tablets. *Polym. Sci.* **2016**, *2*. [[CrossRef](#)]
14. Konta, A.; García-Piña, M.; Serrano, D. Personalised 3D Printed Medicines: Which Techniques and Polymers Are More Successful? *Bioengineering* **2017**, *4*, 79. [[CrossRef](#)] [[PubMed](#)]
15. Norman, J.; Madurawe, R.D.; Moore, C.M.V.; Khan, M.A.; Khairuzzaman, A. A new chapter in pharmaceutical manufacturing: 3D-printed drug products. *Adv. Drug Deliv. Rev.* **2017**, *108*, 39–50. [[CrossRef](#)] [[PubMed](#)]
16. Khaled, S.A.; Burley, J.C.; Alexander, M.R.; Yang, J.; Roberts, C.J. 3D printing of five-in-one dose combination polypill with defined immediate and sustained release profiles. *J. Control. Release* **2015**, *217*, 308–314. [[CrossRef](#)] [[PubMed](#)]
17. Goyanes, A.; Robles Martinez, P.; Buanz, A.; Basit, A.W.; Gaisford, S. Effect of geometry on drug release from 3D printed tablets. *Int. J. Pharm.* **2015**, *494*, 657–663. [[CrossRef](#)] [[PubMed](#)]
18. Kadry, H.; Al-Hilal, T.A.; Keshavarz, A.; Alam, F.; Xu, C.; Joy, A.; Ahsan, F. Multi-purposable filaments of HPMC for 3D printing of medications with tailored drug release and timed-absorption. *Int. J. Pharm.* **2018**, *544*, 285–296. [[CrossRef](#)] [[PubMed](#)]
19. Sadia, M.; Isreb, A.; Abbad, I.; Isreb, M.; Aziz, D.; Selo, A.; Timmins, P.; Alhnan, M.A. From ‘fixed dose combinations’ to ‘a dynamic dose combiner’: 3D printed bi-layer antihypertensive tablets. *Eur. J. Pharm. Sci.* **2018**, *123*, 484–494. [[CrossRef](#)] [[PubMed](#)]
20. Wang, J.; Goyanes, A.; Gaisford, S.; Basit, A.W. Stereolithographic (SLA) 3D printing of oral modified-release dosage forms. *Int. J. Pharm.* **2016**, *503*, 207–212. [[CrossRef](#)]
21. Feuerbach, T.; Kock, S.; Thommes, M. Characterisation of fused deposition modeling 3D printers for pharmaceutical and medical applications. *Pharm. Dev. Technol.* **2018**, *23*, 1136–1145. [[CrossRef](#)]
22. Tran, T.Q.; Chinnappan, A.; Lee, J.K.Y.; Loc, N.H.; Tran, L.T.; Wang, T.; Vijay Kumar, V.; Jayathilaka, W.A.D.M.; Ji, D.; Doddamani, M.; et al. 3D Printing of Highly Pure Copper. *Metals* **2019**, *9*, 756. [[CrossRef](#)]
23. Goyanes, A.; Wang, J.; Buanz, A.; Martínez-Pacheco, R.; Telford, R.; Gaisford, S.; Basit, A.W. 3D Printing of Medicines: Engineering Novel Oral Devices with Unique Design and Drug Release Characteristics. *Mol. Pharm.* **2015**, *12*, 4077–4084. [[CrossRef](#)]
24. Skowyra, J.; Pietrzak, K.; Alhnan, M.A. Fabrication of extended-release patient-tailored prednisolone tablets via fused deposition modelling (FDM) 3D printing. *Eur. J. Pharm. Sci.* **2015**, *68*, 11–17. [[CrossRef](#)] [[PubMed](#)]
25. Rahman, Z.; Barakh Ali, S.F.; Ozkan, T.; Charoo, N.A.; Reddy, I.K.; Khan, M.A. Additive Manufacturing with 3D Printing: Progress from Bench to Bedside. *AAPS J.* **2018**, *20*, 101. [[CrossRef](#)] [[PubMed](#)]
26. Solanki, N.G.; Tahsin, M.; Shah, A.V.; Serajuddin, A.T.M. Formulation of 3D Printed Tablet for Rapid Drug Release by Fused Deposition Modeling: Screening Polymers for Drug Release, Drug-Polymer Miscibility and Printability. *J. Pharm. Sci.* **2018**, *107*, 390–401. [[CrossRef](#)] [[PubMed](#)]
27. Alhnan, M.A.; Okwuosa, T.C.; Sadia, M.; Wan, K.-W.; Ahmed, W.; Arafat, B. Emergence of 3D Printed Dosage Forms: Opportunities and Challenges. *Pharm. Res.* **2016**, *33*, 1817–1832. [[CrossRef](#)] [[PubMed](#)]
28. Modica de Mohac, L.; Keating, A.; de Fátima Pina, M.; Raimi-Abraham, B. Engineering of Nanofibrous Amorphous and Crystalline Solid Dispersions for Oral Drug Delivery. *Pharmaceutics* **2018**, *11*, 7. [[CrossRef](#)] [[PubMed](#)]
29. Goyanes, A.; Buanz, A.B.M.; Hatton, G.B.; Gaisford, S.; Basit, A.W. 3D printing of modified-release aminosaliclylate (4-ASA and 5-ASA) tablets. *Eur. J. Pharm. Biopharm.* **2015**, *89*, 157–162. [[CrossRef](#)]
30. Goyanes, A.; Buanz, A.B.M.; Basit, A.W.; Gaisford, S. Fused-filament 3D printing (3DP) for fabrication of tablets. *Int. J. Pharm.* **2014**, *476*, 88–92. [[CrossRef](#)]
31. Tagami, T.; Fukushige, K.; Ogawa, E.; Hayashi, N.; Ozeki, T. 3D Printing Factors Important for the Fabrication of Polyvinylalcohol Filament-Based Tablets. *Biol. Pharm. Bull.* **2017**, *40*, 357–364. [[CrossRef](#)]
32. Hayes, A.W.; Kruger, C.L. *Hayes’ Principles and Methods of Toxicology*; CRC Press: Boca Raton, FL, USA, 2014.
33. Hassan, S.; Adam, F.; Abu Bakar, M.R.; Abdul Mudalip, S.K. Evaluation of solvents’ effect on solubility, intermolecular interaction energies and habit of ascorbic acid crystals. *J. Saudi Chem. Soc.* **2019**, *23*, 239–248. [[CrossRef](#)]

34. Babagowda Kadadevara Math, R.S.; Goutham, R.; Srinivas Prasad, K. Study of Effects on Mechanical Properties of PLA Filament which is blended with Recycled PLA Materials. *IOP Conf. Ser. Mater. Sci. Eng.* **2018**, *310*, 012103. [[CrossRef](#)]
35. Fell, J.T.; Newton, J.M. Determination of Tablet Strength by the Diametral-Compression Test. *J. Pharm. Sci.* **1970**, *59*, 688–691. [[CrossRef](#)] [[PubMed](#)]
36. Banić-Tomišić, Z.; Kojić-Prodić, B.; Širola, I. Hydrogen bonds in the crystal packings of mesalazine and mesalazine hydrochloride. *J. Mol. Struct.* **1997**, *416*, 209–220. [[CrossRef](#)]
37. Groom, C.R.; Bruno, I.J.; Lightfoot, M.P.; Ward, S.C. The Cambridge Structural Database. *Acta Crystallogr. Sect. B Struct. Sci. Cryst. Eng. Mater.* **2016**, *72*, 171–179. [[CrossRef](#)] [[PubMed](#)]
38. Michael ARepka Nigel Langley, J.D. *Melt Extrusion: Materials, Technology and Drug Product Design* (AAPS Advances in the Pharmaceutical Sciences Series Book; Springer Science & Business Media: Berlin, Germany, 2013. [[CrossRef](#)]
39. Wlodarski, K.; Zhang, F.; Liu, T.; Sawicki, W.; Kipping, T. Synergistic Effect of Polyvinyl Alcohol and Copovidone in Itraconazole Amorphous Solid Dispersions. *Pharm. Res.* **2018**, *35*, 16. [[CrossRef](#)]
40. Konno, H.; Handa, T.; Alonzo, D.E.; Taylor, L.S. Effect of polymer type on the dissolution profile of amorphous solid dispersions containing felodipine. *Eur. J. Pharm. Biopharm.* **2008**, *70*, 493–499. [[CrossRef](#)]
41. Konno, H.; Taylor, L.S. Influence of Different Polymers on the Crystallization Tendency of Molecularly Dispersed Amorphous Felodipine. *J. Pharm. Sci.* **2006**, *95*, 2692–2705. [[CrossRef](#)]
42. Gupta, D.; Jassal, M.; Agrawal, A.K. The electrospinning behavior of poly(vinyl alcohol) in DMSO–water binary solvent mixtures. *RSC Adv.* **2016**, *6*, 102947–102955. [[CrossRef](#)]
43. Paruta, A.N.; Sciarone, B.J.; Lordi, N.G. Correlation between solubility parameters and dielectric constants. *J. Pharm. Sci.* **1962**, *51*, 704–705. [[CrossRef](#)]
44. ThermoFisher. *Kaolin Asp<sup>®</sup> 400p Safety Data Sheet*; Emirates U.A.: Fair Lawn, NJ, USA, 2012; pp. 8–10.
45. Åkerlöf, G. Dielectric constants of some organic solvent-water mixtures at various temperatures. *J. Am. Chem. Soc.* **1932**, *54*, 4125–4139. [[CrossRef](#)]
46. Chernyak, Y. Dielectric constant, dipole moment, and solubility parameters of some cyclic acid esters. *J. Chem. Eng. Data* **2006**, *51*, 416–418. [[CrossRef](#)]
47. Mohsin, M.; Hossin, A.; Haik, Y. Thermomechanical properties of poly(vinyl alcohol) plasticized with varying ratios of sorbitol. *Mater. Sci. Eng. A* **2011**, *528*, 925–930. [[CrossRef](#)]
48. Goyanes, A.; Chang, H.; Sedough, D.; Hatton, G.B.; Wang, J.; Buanz, A.; Gaisford, S.; Basit, A.W. Fabrication of controlled-release budesonide tablets via desktop (FDM) 3D printing. *Int. J. Pharm.* **2015**, *496*, 414–420. [[CrossRef](#)] [[PubMed](#)]
49. Choi, J.; Jang, B.N.; Park, B.J.; Joung, Y.K.; Han, D.K. Effect of Solvent on Drug Release and a Spray-Coated Matrix of a Sirolimus-Eluting Stent Coated with Poly(lactic-co-glycolic acid). *Langmuir* **2014**, *30*, 10098–10106. [[CrossRef](#)] [[PubMed](#)]
50. Raimi-Abraham, B.T.; Mahalingam, S.; Edirisinghe, M.; Craig, D.Q.M. Generation of poly(*N*-vinylpyrrolidone) nanofibres using pressurised gyration. *Mater. Sci. Eng. C* **2014**, *39*, 168–176. [[CrossRef](#)] [[PubMed](#)]
51. Modica de Mohac, L.; de Fátima Pina, M.; Raimi-Abraham, B.T. Solid microcrystalline dispersion films as a new strategy to improve the dissolution rate of poorly water soluble drugs: A case study using olanzapine. *Int. J. Pharm.* **2016**, *508*, 42–50. [[CrossRef](#)]
52. Sun, D.D.; Lee, P.I. Probing the mechanisms of drug release from amorphous solid dispersions in medium-soluble and medium-insoluble carriers. *J. Control. Release* **2015**, *211*, 85–93. [[CrossRef](#)]
53. Baghel, S.; Cathcart, H.; O'Reilly, N.J. Polymeric Amorphous Solid Dispersions: A Review of Amorphization, Crystallization, Stabilization, Solid-State Characterization, and Aqueous Solubilization of Biopharmaceutical Classification System Class II Drugs. *J. Pharm. Sci.* **2016**, *105*, 2527–2544. [[CrossRef](#)]
54. Sun, D.D.; Lee, P.I. Evolution of Supersaturation of Amorphous Pharmaceuticals: The Effect of Rate of Supersaturation Generation. *Mol. Pharm.* **2013**, *10*, 4330–4346. [[CrossRef](#)]
55. Craig, D.Q.M. The mechanisms of drug release from solid dispersions in water-soluble polymers. *Int. J. Pharm.* **2002**, *231*, 131–144. [[CrossRef](#)]
56. Ilevbare, G.A.; Liu, H.; Edgar, K.J.; Taylor, L.S. Inhibition of solution crystal growth of ritonavir by cellulose polymers—Factors influencing polymer effectiveness. *CrystEngComm* **2012**, *14*, 6503. [[CrossRef](#)]

57. Megrab, N.A.; Williams, A.C.; Barry, B.W. Oestradiol permeation through human skin and silastic membrane: Effects of propylene glycol and supersaturation. *J. Control. Release* **1995**, *36*, 277–294. [[CrossRef](#)]
58. Curatolo, W.; Nightingale, J.A.; Herbig, S.M. Utility of Hydroxypropylmethylcellulose Acetate Succinate (HPMCAS) for Initiation and Maintenance of Drug Supersaturation in the GI Milieu. *Pharm. Res.* **2009**, *26*, 1419–1431. [[CrossRef](#)] [[PubMed](#)]



© 2019 by the authors. Licensee MDPI, Basel, Switzerland. This article is an open access article distributed under the terms and conditions of the Creative Commons Attribution (CC BY) license (<http://creativecommons.org/licenses/by/4.0/>).